

## Observation of vibrational modes of irregular drums

Olivier Haeberlé<sup>a)</sup> and Bernard Sapoval<sup>b)</sup>

Laboratoire de Physique de la Matière Condensée, CNRS-Ecole Polytechnique, F-91128 Palaiseau Cédex, France

Kristen Menou and Holger Vach

Laboratoire d'Optique Quantique, CNRS-Ecole Polytechnique, F-91128 Palaiseau Cédex, France

(Received 13 July 1998; accepted for publication 6 October 1998)

Vibrational modes of irregular or prefractal drums have been calculated using a correspondence between the wave propagation and the diffusion equations. The resonance frequencies and the vibrational-mode structures measured on low thickness plastic film membranes using a holographic setup are found to be in good agreement with theoretical predictions. © 1998 American Institute of Physics. [S0003-6951(98)03949-7]

Vibrational properties of irregular objects are of general interest but remain largely unexplained. Fractal geometry has appeared to be an efficient tool to describe irregularity.<sup>1</sup> When the physical properties of an object are due to the hierarchical character of its geometry, the main physical characteristics can be found by studying deterministic fractals.<sup>2</sup> The problem we address here is the vibration of drums with irregular boundaries. The main properties of resonators are their spectra, the structure of their vibrational modes and the damping of these modes. Mathematical aspects of the excitation of fractal drums are examined in Refs. 3 and 4.

The drums we study are described in Fig. 1. On top, the generator used to “fractalize” the square initiator No. 0 is shown. Drum No. 1 is a regular prefractal of the first generation. It has a C4 symmetry and the corresponding degeneracies. Drum No. 2 is obtained from drum No. 0 by applying the generator on two neighboring sides only. Drum No. 3 is similar to drum No. 1 but its generator has unequal length segments. The two latter drums are not symmetric and, therefore, have no spectral degeneracy, except for possible accidental degeneracies.

We computed the eigenfrequencies and the vibrational-mode structures of the drums using a correspondence between the wave propagation equation and the diffusion equation:<sup>5,6</sup>

$$\Delta\Psi = (1/c^2)\partial^2\Psi/\partial t^2, \quad (1)$$

$$D\Delta\Psi = \partial\Psi/\partial t. \quad (2)$$

Here,  $c$  is the wave velocity and  $D$  is the diffusion coefficient. The general solution of propagation Eq. (1) is made out of imaginary exponentials, whereas the solution of diffusion Eq. (2) is made out of decaying real exponentials. However, when solved on the same domain, the two problems lead to the same eigenvalue and eigenfunction problem through the relation:

$$(D\tau_n)^{-1} = \omega_n^2/c^2. \quad (3)$$

Here,  $\tau_n$  is the decay time constant of the diffusion eigenstate  $\Psi_n$  and  $\omega_n$  is the eigenfrequency of the corresponding vibration mode. Details about the numerical method used to solve Eq. (2) can be found in Refs. 5 and 6.

In Table I, we give the ten first eigenfrequencies computed from Eq. (2) for the various drums shown in Fig. 1. The frequencies have been normalized to the first mode of the square drum. Note that the eigenfrequencies are shifted to higher values: everything happens as if the effective membrane was smaller, although the area is conserved in the process.

In Fig. 2, we show the shape of some of the computed modes. The amplitudes are represented by gray levels, black standing for regions with large positive amplitudes and white standing for regions with large negative amplitudes. The fundamental mode of each structure exhibits no nodal lines and its amplitude decays rapidly from the center towards the edges.<sup>7</sup> Modes 2 and 3 of drum No. 1 are degenerated and one obtains the third mode by a 90° rotation of the second mode. Of particular interest is the sixth mode of drum No. 3. It is localized in the upper-left “wing” of the structure and a large part of the drum does not vibrate, or vibrates with a very small amplitude. It is a case of weak localization which

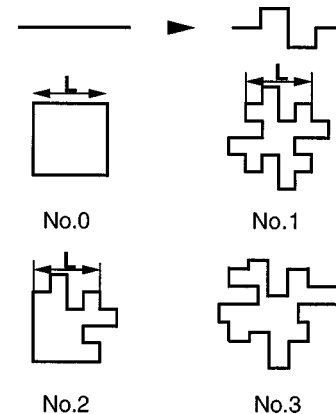


FIG. 1. Top: Generator of the fractal drums. Drum Nos. 0 and 1 are prefractals at iteration 0 and 1. Drum No. 2 is obtained by applying the generator only on two neighboring sides of the square initiator. Drum No. 3 is built with an irregular generator with segments of lengths 0.5, 1, and 1.5  $\times (L/4)$ .

<sup>a)</sup>Present address: Laboratoire LAB.EL, Université de Haute-Alsace, IUT, 61 rue Albert Camus, F-68093 Mulhouse Cedex, France.

<sup>b)</sup>Electronic mail: bernard.sapoval@polytechnique.fr

TABLE I. Relative eigenfrequencies of the four drums shown in Fig. 1. Frequencies are normalized to the fundamental eigenfrequency of the square drum No. 0.

Mode	Drum No. 0	Drum No. 1	Drum No. 2	Drum No. 3
1	1	1.8253	1.2432	1.6595
2	1.5811	2.5016	1.7942	2.1586
3	1.5811	2.5016	2.0509	2.4865
4	2	2.5617	2.2742	2.6820
5	2.2361	2.6326	2.5177	2.8151
6	2.2361	2.9578	2.6313	2.8542
7	2.5495	2.9578	2.8809	3.1184
8	2.5495	3.3205	2.9072	3.2862
9	2.9155	3.4492	2.9790	3.3247
10	2.9155	3.4804	3.2220	3.3784

is often observed in surface fractal resonators.<sup>5,6</sup>

The drum contours have been made by laser machining in stainless-steel plates (thickness 0.5 mm). The membranes are made out of 5  $\mu\text{m}$  thick stretched polyethylene films. To ensure uniform tension, one starts from a square piece of film which is much larger than the plates. The film is stretched in all directions to increase its size, but keeping its square shape. The steel plate is then glued on the central part of the film, where the tension is expected to be the most uniform. We verified the tension uniformity by examining the drums between crossed polarizers: birefringence may appear in some parts of the membrane submitted to a nonuniform surface tension. None was observed with our apparatus. In order to use the drums in a holographic setup, the surfaces of the transparent membranes are made diffusive by spreading small silica particles (40–60  $\mu\text{m}$ ) onto them and softly fixing these particles with a thin layer of hair spray. This increases the mass of the membrane. Measurements before and after spreading the particles have shown that the eigenfrequencies

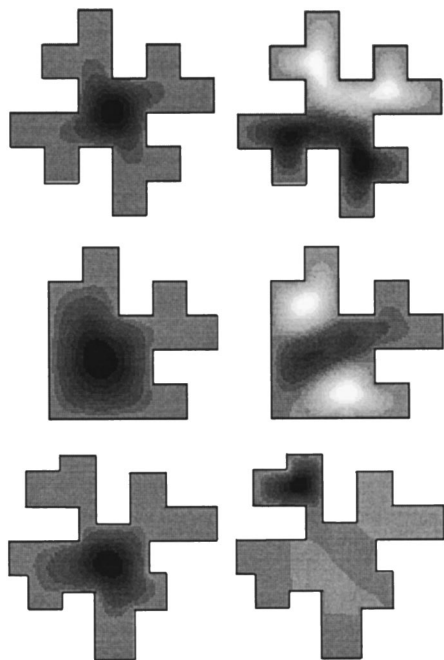


FIG. 2. Top: modes 1 and 2 of drum No. 1. Middle: modes 1 and 4 of drum No. 2. Bottom: modes 1 and 6 of drum No. 3. Note that the mode 2 of drum No. 1 is not coupled to a uniform excitation.

TABLE II. Experimentally identified resonances of drum Nos. 1 and 3. A slash bar indicates a nonobserved resonance. For each drum, eigenfrequencies are given relative to the fundamental and they are compared to theoretical predictions (in parentheses).

Mode	Drum No. 1		Drum No. 3	
	$\nu$ (Hz)	$\nu/\nu_1$	$\nu$ (Hz)	$\nu/\nu_1$
1	298.0 $\pm$ 1	1(1)	146.0 $\pm$ 1	1(1)
2	/	/(1.37)	/	/(1.30)
3	/	/(1.37)	219.9 $\pm$ 1	1.51(1.50)
4	/	/(1.41)	/	/(1.62)
5	/	/(1.45)	243.7 $\pm$ 1	1.67(1.69)
6	485.0 $\pm$ 1	1.62(1.63)	/	/(1.72)
7	/	1.62(1.63)	275.9 $\pm$ 1	1.89(1.88)
8	541.7 $\pm$ 1	1.82(1.82)	/	/(1.98)
9	563.4 $\pm$ 1	1.89(1.90)	293.4 $\pm$ 1	2.01(2.00)

are slightly shifted to lower values, but their ratios remain constant.

The drums are excited by a loudspeaker installed at about 1 m distance, to ensure an almost uniform excitation. To avoid possible nonlinear effects, the excitation is kept as low as possible. To find the resonances experimentally a laser beam hits the nondiffusive face of the membrane and we observe the reflected laser spot on a screen some 2 m away. At resonance, the vibrational amplitude greatly increases and the laser spot distinctly oscillates. Alternatively, we use an accelerometer placed in front of the membrane. The membrane pushes and pulls the air, which applies forces on the accelerometer. While scanning the loudspeaker frequency, the electrical tension delivered by the accelerometer is recorded using a lock-in amplifier. Both methods gave the same results for the eigenfrequencies and the spectral widths of the resonances.

In Table II, we give some observed resonances for drums No. 1 and 3. Results are given in reduced units, taking as a natural unit the fundamental of each drum. Numbers in parenthesis are theoretical values. Table II shows that we identified several modes for each drum with a fairly good precision ( $\Delta\nu/\nu \leq 2\%$ ). Some resonances were not observed, probably because of a weak coupling of the drums with the excitation sound wave: due to the symmetry of drum No. 1 the eigenstates 2, 3, and 4 are not expected to be coupled to a uniform excitation.<sup>5</sup> The resonance widths are of the order of 1 Hz, showing that the  $Q$  factors are of the same order for all observed modes. Losses are of two kinds: those due to energy dissipation in the membrane itself, and those due to coupling with air (a vibrating membrane is a loudspeaker). In our case, the latter is probably dominant.

We use a standard holographic Mach–Zehnder setup<sup>8</sup> to record the vibrational modes of the drums with a time-average method. For a sinusoidal movement with maximal amplitude  $A$  of the object, the intensity distribution over the surface of the reconstructed object in the hologram, when the illumination time is much larger than the vibrational period, is given by<sup>8</sup>

$$I(x, y) \propto J_0^2[2\pi AF(x, y)(\cos \varphi_1 + \cos \varphi_2)/\lambda]. \quad (4)$$

Here,  $\lambda$  is the wavelength of the laser beam,  $J_0$  is the zeroth-order Bessel function of the first kind,  $\varphi_1$  is the angle between the direction of illumination and the direction of the

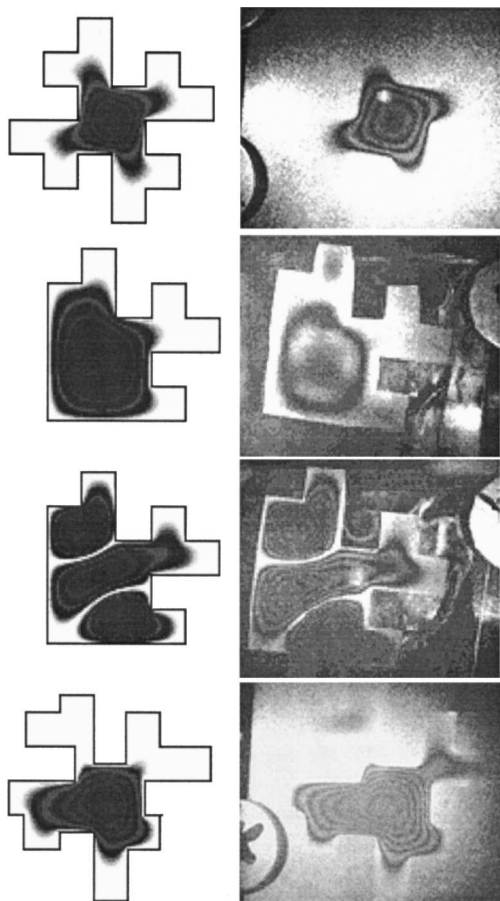


FIG. 3. Comparison of some simulations using Eq. (4) with  $A=1\ \mu\text{m}$ ,  $\varphi_1 = \varphi_2 = 45^\circ$ ,  $\lambda = 632.8\ \text{nm}$ , and experimental holograms. The number of fringes can be different because amplitudes in the experiments were not precisely adjusted to  $1\ \mu\text{m}$ . The shape of the measured modes compares very favorably with the theory.

displacement,  $\varphi_2$  is the angle between the direction of displacement and the direction of observation, and  $F(x,y)$  describes the vibrational mode. Superposed on the hologram of the membrane appears a set of dark and bright interference fringes following regions with equal vibrational amplitude. Nodal lines separate regions which are vibrating in phase opposition.<sup>7</sup> The number of fringes is proportional to the amplitude of the motion.

The time-average method allows us to measure vibrations with small amplitudes (typically,  $\lambda \ll A \ll 10\lambda$ ), which

requires very low levels of excitation. However, our membranes are very sensitive to excitations produced by air flows and noise because of their small thickness and weight. Temperature effects are also noticeable: a change of  $5^\circ\text{C}$  in the room temperature shifts the resonance frequencies by several Hz. For these reasons, the optical table was installed in a thermally and acoustically isolated room to avoid excitation of the membrane by stray noise and to guarantee reproducible experimental conditions. Figure 3 shows experimental holograms recorded at previously measured resonance frequencies. On the left, we show simulations obtained using Eq. (4) with the computed eigenstates. The comparison is very favorable and is an indicator of the good quality of the membranes.

The results we obtained also validate the use of our method to compute vibrational eigenfrequencies and eigenmodes of irregular drums using the diffusion equation instead of the wave propagation equation. Our membranes were acoustically excited. Therefore, we could not perform the experiments in vacuum. As a consequence, the energy losses are mainly due to the coupling with air and it was not possible to study the intrinsic damping properties of our membranes. Increased irregularity could increase the internal losses of a membrane because large differences in vibrational amplitude occur on small scales, possibly inducing nonlinear effects.<sup>5</sup> Liquid-crystal membranes which are of excellent quality can be electrically excited. They can vibrate in vacuum and appear very promising to study the localization effects.<sup>9</sup>

The holographic measurements were made at the acoustic room of the Centre de Travaux Expérimentaux of the Ecole Polytechnique. The authors wish to thank P. Lavielle for his help in recording the photographs.

<sup>1</sup>B. B. Mandelbrot, *The Fractal Geometry of Nature* (Freeman, San Francisco, CA, 1982).

<sup>2</sup>B. Sapoval, *Universalités et Fractales* (Flammarion, Paris, 1997).

<sup>3</sup>M. L. Lapidus, J. W. Neuberger, R. J. Renka, and C. A. Griffith, *Int. J. Bifurcation Chaos Appl. Sci. Eng.* **6**, 1185 (1996).

<sup>4</sup>M. Levitin and D. Vassiliev, *Proc. London Math. Soc.* **72**, 178 (1996).

<sup>5</sup>B. Sapoval and T. Gobron, *Phys. Rev. E* **47**, 3013 (1993).

<sup>6</sup>S. Russ, B. Sapoval, and O. Haeberlé, *Phys. Rev. E* **55**, 1413 (1997).

<sup>7</sup>D. Courant and D. Hilbert, *Methods of Mathematical Physics* (Interscience, New York, 1965).

<sup>8</sup>Y. I. Ostrovsky, M. M. Butusov, and G. V. Ostrovskaya, *Interferometry by Holography* (Springer, Berlin, 1980).

<sup>9</sup>A. Pieranski (private communication).